nature neuroscience

Ephrin-As mediate targeting of eye-specific projections to the lateral geniculate nucleus

Andrew D Huberman[1,4], Karl D Murray[1], David K Warland[1,2], David A Feldheim[3] & Barbara Chapman[1,2]

Axon guidance cues contributing to the development of eye-specific visual projections to the lateral geniculate nucleus (LGN) have not previously been identified. Here we show that gradients of ephrin-As and their receptors (EphAs) direct retinal ganglion cell (RGC) axons from the two eyes into their stereotyped pattern of layers in the LGN. Overexpression of EphAs in ferret RGCs using *in vivo* electroporation induced axons from both eyes to misproject within the LGN. The effects of EphA overexpression were competition-dependent and restricted to the early postnatal period. These findings represent the first demonstration of eye-specific pathfinding mediated by axon guidance cues and, taken with other reports, indicate that ephrin-As can mediate several mapping functions within individual target structures.

In mammals, retinal ganglion cell (RGC) axons are segregated into eye-specific layers in the lateral geniculate nucleus (LGN). Early in development, however, retinogeniculate axons from the two eyes are intermingled[1–3]. The segregation of eye-specific projections into layers is an established model system for studying axon targeting during development[4]. Technically, the term "layers" refers to discrete cellular groupings. However, "eye-specific LGN layers" is also used to refer to the regions of stereotyped size, shape and position formed by RGC axons arising from each eye. (Hereafter we use the term "layers" only in this latter sense.) The regularity of eye-specific layers is a distinguishing feature of mammalian brains; their spatial arrangement is different between, but invariant within, species[5]. In carnivores such as cats and ferrets, layer A contains axons from the contralateral eye and always resides in the inner portion of the LGN, whereas layer A1 contains axons from the ipsilateral eye and always resides in the outer LGN[5]. This invariance is in bold contrast to eye-specific projections found elsewhere along the visual pathway, such as eye-specific patches in the superior colliculus (SC)[6] or ocular dominance columns in visual cortex[7], which vary tremendously across individuals of a given species in terms of their size, shape and position.

Numerous studies have shown that altering neural activity perturbs eye-specific retinogeniculate segregation[8–12]. However, the invariant positioning of eye-specific LGN layers cannot be explained by purely activity-dependent mechanisms[13,14] and recent data have challenged the idea that neural activity plays a direct, instructive role in segregation of eye-specific projections to the LGN[15]. Non-activity-based explanations for patterning of eye-specific layers have been proposed, such as the differential arrival time of axons from the contralateral versus ipsilateral eye[13,16,17]. Unfortunately, timing of ingrowth is a difficult variable to manipulate, so this hypothesis has never been directly tested. Another hypothesis is that axon guidance cues mediate patterning of eye-specific layers[10,15,18–21], but a direct role for axon guidance cues in the development of eye-specific connectivity has not previously been reported.

What sort of axon guidance cue might regulate patterning of eye-specific layers? In mammals with highly developed binocular vision such as carnivores and primates, each "eye-specific" layer receives RGC axons strictly from either the nasal portion of the contralateral retina or the temporal portion of the ipsilateral retina. Indeed, in the LGN of achiasmatic carnivores, axons arising from the nasal retina segregate from those arising from the temporal retina of the same eye, into regions identical to layers A and A1 (ref. 21). Also, animals with coat-color mutations, despite having aberrant RGC axon decussation patterns at the optic chiasm, still segregate nasal axons from temporal axons within the LGN[22,23]. These observations indicate that the nasal-retina versus temporal-retina distinction (as opposed to the left-eye versus right-eye distinction) is the key parameter for patterning of eye-specific projections in the LGN. Numerous experiments carried out in lower vertebrates and mice indicate that ephrin-As mediate retinotopic mapping of the nasal-temporal axis in the SC and LGN[24–30]. We wanted to test whether ephrin-As have a second function in retinogeniculate mapping: dictating the stereotyped patterning of the eye-specific LGN layers. We decided to address this question in ferrets because, unlike in mice[31,32], eye-specific layers in ferrets obey the nasal- versus temporal-retina distinction[33], and retinotopic mapping and eye segregation occur during distinct stages of development[34–36].

In the normal development of eye-specific retinogeniculate projections in the ferret (**Fig. 1a**,**b**), retinal innervation of the LGN occurs from embryonic day (E) 27 until roughly E40 (ferret gestation = 42 d)[37]. Retinotopic mapping is already adult-like at birth in this species; axons that convey information from the same location

[1]Center for Neuroscience, 1544 Newton Ct., University of California, Davis, California 95616, USA. [2]Section of Neurobiology, Physiology and Behavior, 1 Shields Ave., University of California, Davis, California 95616, USA. [3]Department of Molecular, Cellular and Developmental Biology, 225 Sinsheimer Labs, University of California Santa Cruz, Santa Cruz, California 95064, USA. [4]Present address: Department of Neurobiology, Fairchild Building, Stanford University School of Medicine, Palo Alto, California 94305, USA. Correspondence should be addressed to B.C. (bxchapman@ucdavis.edu).

Published online 17 July 2005; doi:10.1038/nn1505

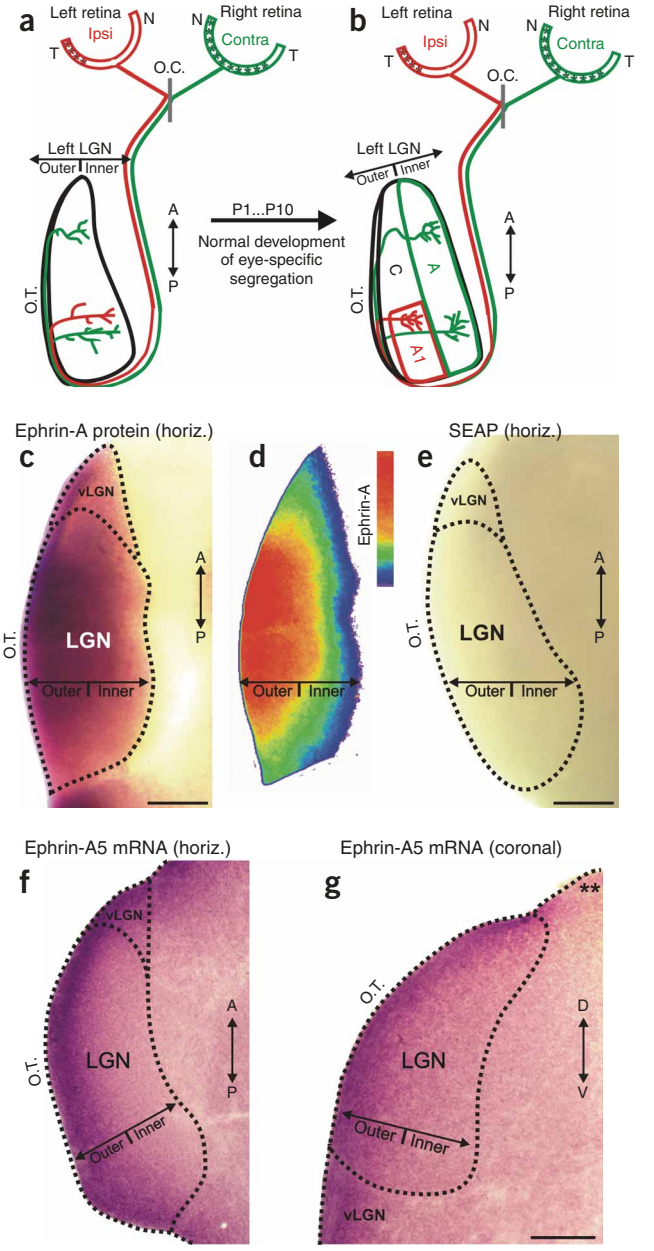

Figure 1 Eye-specific development and ephrin-As in the ferret LGN. (**a**,**b**) Schematic diagram of RGC axon ingrowth and arborization during eye-specific segregation in the P1 and P10 LGN. Horizontal plane is shown and, for simplicity, only the retinal projection to the left LGN is shown. Asterisks (in the retinas) indicate the location of contralateral and ipsilateral RGCs that project to the left LGN. O.C., optic chiasm; T, temporal pole; N, nasal pole; A, contralateral eye layer; A1, ipsilateral eye layer; C, nonprincipal layers; A/P, anterior-posterior axis; O.T., optic tract. (**c**) Expression of pan-ephrin-A protein in a horizontal section of the P3 ferret LGN. (**d**) Color-scaled densitometry plot of ephrin-A protein in the P3 LGN. (**e**) Secreted embryonic alkaline phosphatase (SEAP)-AP shows no staining in the P3 ferret LGN. (**f**) Outer > inner gradient of ephrin-A5 mRNA expression in horizontal section of the P0 ferret LGN. (**g**) Outer > inner gradient of ephrin-A5 mRNA seen in a coronal plane section of the P1 ferret LGN. Asterisks indicate an edge of the same tissue section that does not exhibit dioxigenin (DIG) labeling, indicating that the outer > inner gradient in the LGN is not due to edge artifacts. D-V, dorsal-ventral axis; vLGN, ventral lateral geniculate nucleus. Scale bars, 150 μm (**c**–**g**).

in visual space terminate along a common line of projection, which extends along the outer-inner axis of the LGN[34,35]. The line of decussation (contralateral versus ipsilateral projection pattern of RGC axons at the optic chiasm) is also adult-like at birth[33]. The binocular overlap in the LGN on postnatal day 0 (P0) is due to RGC axons extending rudimentary arborizations at multiple locations along the outer-inner axis of the LGN and ipsilateral eye axons projecting, along with contralateral eye axons, to the inner limit of the LGN (**Fig. 1a**)[2,20,38]. Eye-specific segregation is completed by P10 (refs. 2,20,38). This process reflects (i) the elimination of inappropriate arborizations found along RGC axon shafts, (ii) the retraction of ipsilateral eye arborizations from the inner LGN, (iii) the elaboration of ipsilateral eye arborizations in the outer LGN and (iv) the elaboration of contralateral eye arborizations in the inner LGN (**Fig. 1b**)[38,39].

Here we show that, during the period of eye-specific segregation, EphAs are differentially expressed in the contralateral-eye RGC axons versus ipsilateral-eye RGC axons that converge on the same line of projection. We also show that ephrin-As are distributed in an outer-greater-than-inner (outer > inner) gradient within the LGN. This arrangement should promote the characteristic contralateral:inner, ipsilateral:outer mapping of RGC axons to the principal (A and A1) layers of the LGN. EphA overexpression in RGCs using *in vivo* electroporation supported this hypothesis, forcing axons from both eyes to project into the inappropriate eye-specific regions of the LGN. EphA overexpression did not alter levels or patterns of spontaneous retinal activity. Thus, ephrin-A:EphA interactions directly mediate targeting of eye-specific retinogeniculate projections through their effects on axon guidance.

RESULTS

EphA and Ephrin-A expression in postnatal visual system

We first used affinity-probe binding of EphA3 linked to alkaline phosphatase (EphA3-AP) to detect all the ephrin-A proteins[40] in the ferret LGN. Ephrin-A proteins were seen in an outer > inner gradient in the LGN (**Fig. 1c**,**d**). No staining was evident in LGNs treated with AP alone (**Fig. 1e**). We also performed *in situ* hybridization to detect ephrin-A5 mRNA[28–30,41]. This confirmed the presence of an outer > inner gradient of ephrin-A5 mRNA in the LGN that could be seen in both the horizontal (**Fig. 1f**) and coronal (**Fig. 1g**) planes. The outer > inner gradient was not simply a consequence of edge artifacts; ephrin-A5 gradients were also observed in more medial-residing thalamic nuclei, such as the ventral-posterior nucleus (not shown), and were consistently absent from non-LGN edges of the same tissue sections (asterisks in **Fig. 1g**). No staining or gradients were observed using sense riboprobe controls (data not shown).

Next we examined the expression of EphAs and ephrinAs in the developing ferret retina. Using an ephrin-A5-AP probe to detect EphA proteins, we observed a central-greater-than-peripheral (central > peripheral) gradient of EphAs within the RGC layer (**Fig. 2a–e**). The lowest densities of EphAs were found at the far-nasal and far-temporal poles, and the highest density of EphAs was found near the central retina (**Fig. 2a–e**). A central > peripheral gradient was present at all dorsal-ventral retinal locations (**Fig. 2e**). We also examined the distribution of EphA5 mRNA by *in situ* hybridization using antisense riboprobes for mouse EphA5 (refs. 28–30) and ferret EphA5. This confirmed the central > peripheral gradient of EphA5 mRNA in the RGC layer (**Fig. 2f**). *In situ* hybridization also showed the presence of a nasal > temporal gradient of mRNA for ephrin-A5 (**Fig. 2g**), which indicates that the central > peripheral expression of EphA5 in the

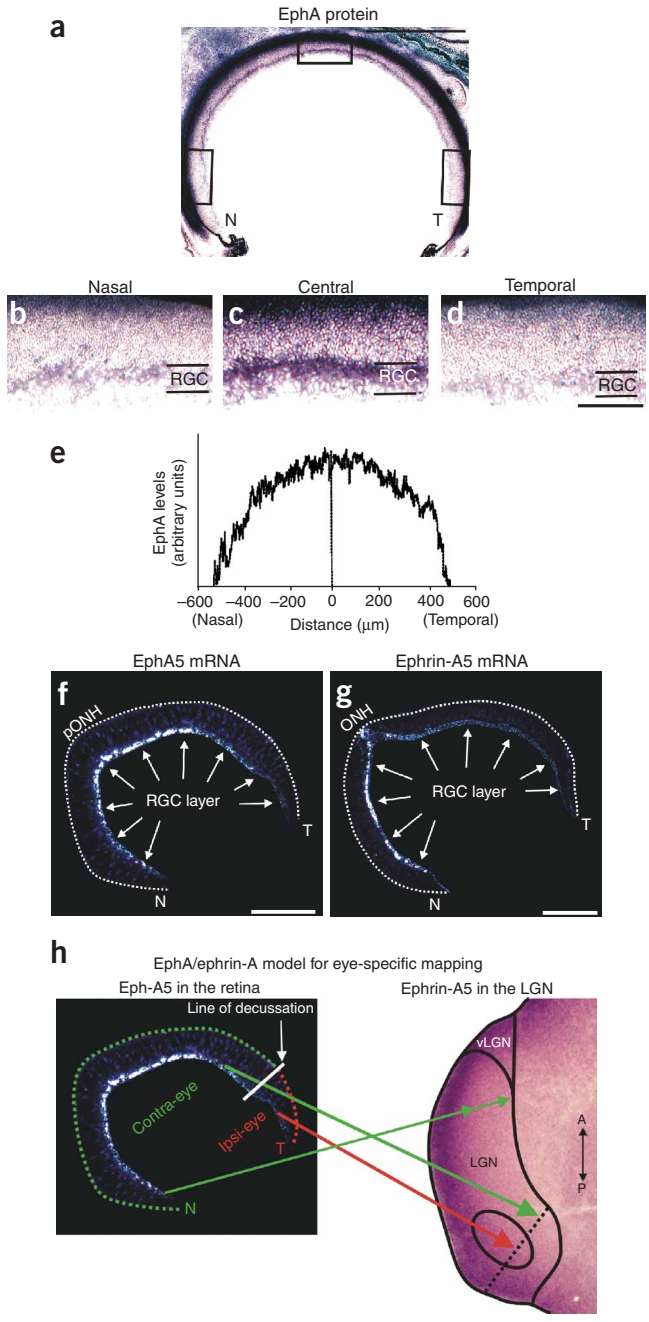

Figure 2 EphAs in the postnatal ferret retina. (**a**) Horizontal section through the P3 ferret retina labeled for pan-EphA protein. Scale bar, 500 μm. (**b**–**d**) High-magnification images of the (**b**) nasal, (**c**) central and (**d**) temporal retina (corresponding to the boxed regions in **a**). RGC, retinal ganglion cell layer. The dark staining at the top of each image is the photoreceptor layer and pigmented epithelium and vasculature. Scale bar, 200 μm (**b**–**d**). (**e**) Densitometry plot of EphA concentrations in the RGC layer along the nasal-temporal axis of the retina, averaged from dorsal-, mid- and ventral-retina sections. (**f**,**g**) *In situ* hybridization with S^{35}-labeled riboprobes, demonstrating (**f**) a central > peripheral gradient of EphA5 mRNA in the P1 ferret retina (horizontal plane) and (**g**) a nasal > temporal gradient of ephrin-A5 mRNA in the P1 ferret retina (also horizontal plane). pONH, peri-optic nerve head; N, nasal pole; T, temporal pole. (**f**,**g**) Dashed line encompasses the neural retina. Scale bar, 250 μm. (**h**) Model for eye-specific mapping of ipsi-projecting RGCs (red arrow) and contra-projecting RGCs (green arrow) from the two eyes, to different locations along a single line of projection (dashed black line) in the LGN. Axons from the far nasal retina (double-headed green arrow) project to multiple locations along the outer-inner axis in the anterior LGN. A single retina is shown only for schematic purposes; in reality the contralaterally projecting axons and the ipsilateral projecting axons that converge on the same line of projection in the LGN arise from opposite retinas.

retina (**Fig. 2f**) is not simply due to lower RGC densities in the peripheral versus central retina. The nasal > temporal expression of ephrin-A5 (**Fig. 2g**) may also have implications for mapping of retinal projections to the LGN[42].

Ephrin-A model for eye-specific targeting

Ephrin-As have consistently been shown to repel RGC axons expressing relatively higher levels of EphAs[24–30,43]. In the ferret, the temporal-most 12–20% of RGCs do not cross at the chiasm and thereby project to the ipsilateral LGN[32,33]. The central > peripheral gradient of EphAs in the retina means that there are relatively higher levels of EphAs expressed in the RGC axons from the contralateral eye than in the RGC axons from the ipsilateral eye that converge on a the same line of projection in the binocular (posterior) region of the LGN. The outer > inner gradient of ephrin-As in the LGN should therefore repel the contralateral eye axons into the inner LGN (layer A), whereas the ipsilateral eye axons should map to the more outer LGN (layer A1) (**Fig. 2h** and **Supplementary Fig. 1**). Axons from the far-nasal retina of the contralateral eye would still map all along the outer-inner axis in the monocular (anterior) LGN (**Fig. 2h** and **Supplementary Fig. 1**). We did not directly consider the C layers in this study. For clarity, however, C layers are labeled in the photomicrographs and are discussed below.

In vivo electroporation of RGCs

To test whether interactions between ephrin-A and EphA regulate eye-specific layer formation, we developed an electroporation protocol to transfect postnatal ferret RGCs *in vivo* (**Fig. 3a**). Electroporation with control cDNAs encoding green fluorescent protein (GFP) resulted in widespread GFP expression in the RGC layer within 24 h (**Fig. 3b**). Retinal electroporation with GFP on P1 followed by an *in vivo* injection of the anterograde tracer Cholera toxin β-Alexa 594 (red) into the same eye on P10 resulted in complete concordance between the GFP and tracer label on RGC axons within the P10 LGN (**Fig. 3c**,**d**). The GFP/tracer-labeled axons terminated in a pattern normal for the P10 ferret LGN[2,9,10,15,20]. Thus, our electroporation protocol rapidly and stably transfects a large number of RGCs and the transgene is expressed on retinogeniculate axon terminals. Furthermore, our electroporation/transfection protocol does not itself alter patterning of eye-specific retinogeniculate projections.

When we transfected RGCs with EphA3 or EphA5 constructs (EphA3/5) on P1 and then examined the localization of EphA proteins in the retina using ephrin-A5-AP, we observed increased EphA levels in the RGC layer, indicating functional overexpression of EphAs (**Fig. 3e**). EphA3/5 overexpression did not alter RGC density (**Fig. 3f**). To examine EphA overexpression on RGC axons within the LGN, we electroporated the retinas of P1 ferrets with an EphA5:V5 fusion construct (**Supplementary Methods**) and then examined the LGN for expression of the fusion protein, using antibodies directed against the V5 epitope tag. Immunoreactivity for EphA5:V5 was evident throughout the LGN (**Fig. 3g**), indicating that the overexpressed EphA5 protein was trafficked to retinogeniculate axon terminals.

Does EphA overexpression perturb eye-specific targeting?

In P10 ferrets electroporated with control plasmids on P1, normal eye-specific projections to the LGN were observed (**Fig. 4a**). By contrast,

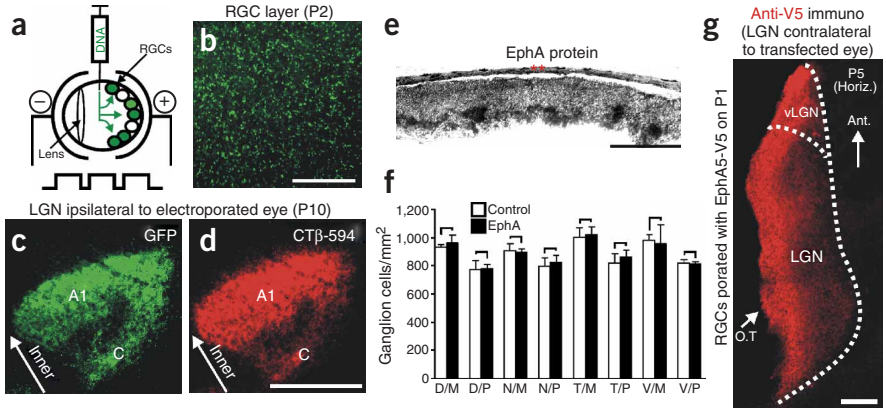

Figure 3 *In vivo* ganglion cell electroporation. (**a**) Diagram of the electroporation procedure. (**b**) Flat-mount view of a P2 retina that was electroporated with GFP on P1. Brightly labeled cell bodies are present throughout the RGC layer. Scale bar, 150 μm. (**c**) GFP-labeled RGC axons in the LGN of a P10 ferret that was monocularly electroporated with GFP on P1. The LGN ipsilateral to the electroporated eye is shown in the horizontal plane; GFP-positive (GFP+) axons are in the normal layer-A1 pattern. The normal ipsilateral C layer is also apparent. (**d**) The GFP-electroporated eye was also injected with choleratoxin β (CTβ-594) to label all RGC axons originating from that eye. (**c**,**d**) Scale bar, 150 μm. (**e**) P10 ferret retina that was transfected with EphA5 on P1 and then processed for ephrin-A5-AP affinity probe binding to detect EphA protein. The far-temporal retina is shown, which normally expresses very low levels of EphAs (see **Fig. 2**). The same result was observed for the far-nasal retina (not shown). Asterisks indicate pigmented epithelium. Scale bar, 200 μm. (**f**) RGC densities from control and EphA-electroporated retinas (paired *t*-test; $n = 4$ retinas per group; error bars represent s.e.m.; D, dorsal; N, nasal; T, temporal; V, ventral; M, mid retina; P, peripheral retina). No significant differences between groups were present at any location. (**g**) Axons expressing an EphA5:V5 fusion construct seen on RGC axons in the LGN of a P5 ferret that was electroporated in the contralateral eye on P1. Scale bar, 200 μm.

P10 ferrets that had been electroporated with EphA3 or EphA5 cDNAs on P1 showed markedly perturbed retinogeniculate projections (**Figs. 4** and **5**) ($n = 14$ ferrets: $n = 7$ EphA3, $n = 7$ EphA5). Most notably, axons from the ipsilateral eye were mistargeted to the inner LGN, into territory normally occupied only by axons from the contralateral eye (**Figs. 4b** and **5b–f**). In addition, axons from the contralateral eye made targeting errors (compare top panels in **Fig. 4a**,**b**). Thus, in contrast to normal and control-electroporated P10 ferrets, in which retinogeniculate inputs are completely segregated into a highly stereotyped pattern of eye-specific layers by P10 (**Fig. 4a**)[2,9,10,15,20], there were severe eye-specific targeting errors and intermingling of contralateral eye and ipsilateral eye axons in the LGN

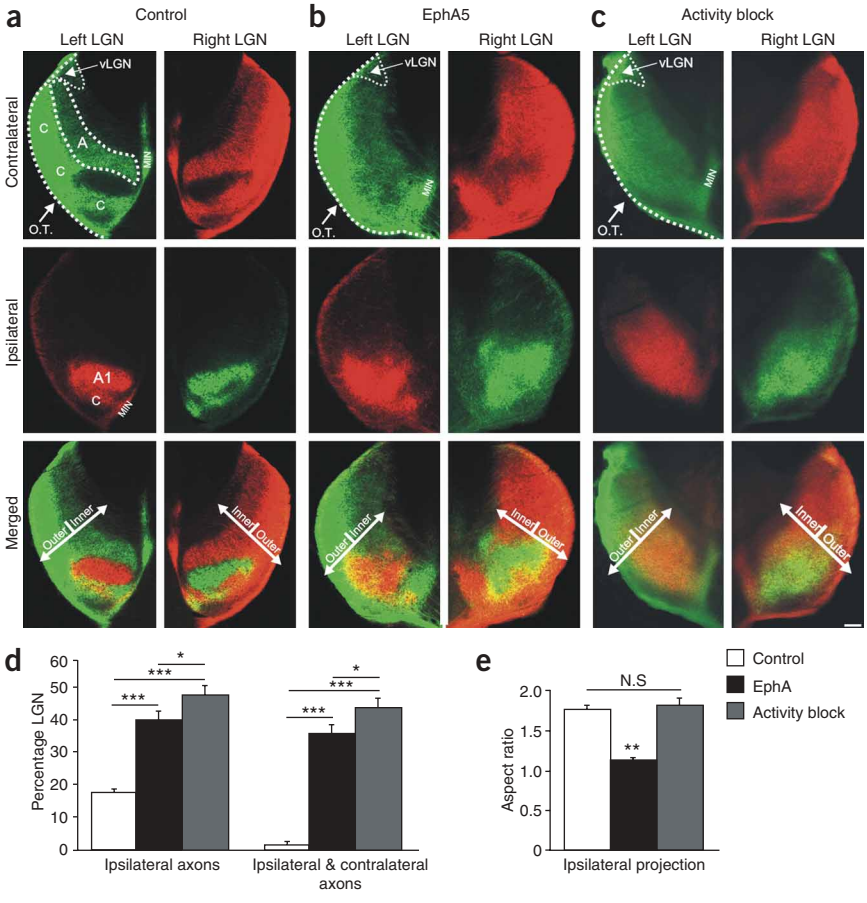

Figure 4 Effect of EphA overexpression on eye-specific targeting and comparison to activity blockade. (**a**–**c**) Contralateral eye inputs (top), ipsilateral eye inputs (middle) and their merged representation (bottom) in the left and right LGNs of (**a**) a P10 control ferret, (**b**) a P10 ferret that was binocularly electroporated with EphA5 on P1 and (**c**) a P10 ferret that had all retinal activity blocked from P1 to P10. Horizontal sections are shown. O.T., optic tract; MIN, medial intralaminar nucleus; vLGN, ventral lateral geniculate nucleus; A, contralateral layer; A1, ipsilateral layer; C, nonprincipal C layers; the boundaries of A and A1 and the optic tract are shown with dashed lines for the left LGN. The outer-inner axis (perpendicular to eye-specific layers) is shown by arrows (merged panels). Scale bar, 100 μm. (**d**) Quantification of the extent of the ipsilateral eye projection area and the degree of binocular intermingling in the LGN. Both EphA overexpression and activity blockade caused significant increases in the area of the LGN containing ipsilateral eye input and the intermingling of ipsi- and contralateral axons, compared to controls (***$P < 0.005$). The effect of activity blockade was significantly greater than the effect of EphA overexpression on both these measures (*$P < 0.05$, unpaired *t*-test; $n = 22$ control cases; $n = 15$ binocular EphA5; $n = 12$ activity blocked). (**e**) Quantification of aspect ratio (long axis:short axis) for ipsilateral eye input to LGN in control ($n = 12$), EphA-transfected ($n = 15$) and retinal activity–blocked ($n = 11$) ferrets. ($P > 0.05$, not significant (N.S.); **$P < 0.01$; *t*-test).

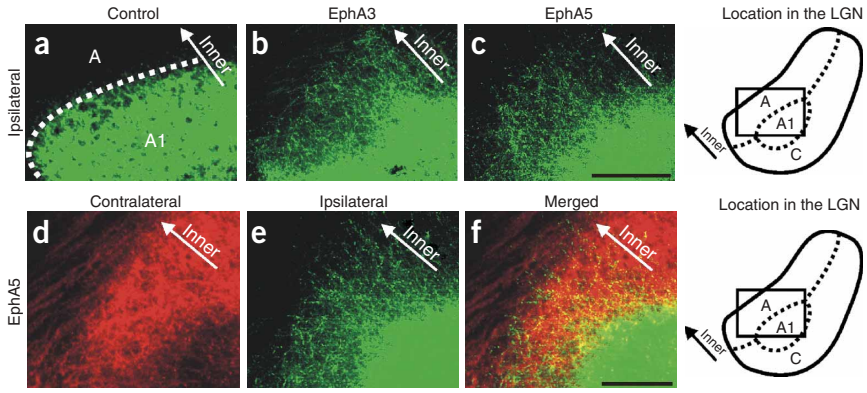

Figure 5 EphA overexpression causes ipsilateral eye axons to misproject into opposite eye territory. (**a**–**c**) Ipsilateral eye inputs to the P10 LGN of (**a**) a control-electroporated ferret, (**b**) a ferret monocularly electroporated with EphA3 and (**c**) a ferret binocularly electroporated with EphA5. (**d**–**f**) In a P10 ferret that was binocularly electroporated with EphA5 on P1, (**d**) contralateral eye axons, (**e**) ipsilateral eye axons and (**f**) their merged representation. Ipsilateral eye expansion into contralateral eye territory was observed here and in every EphA-electroporated ferret examined ($n = 16$ ferrets). Horizontal plane is shown. Scale bars, 100 μm. Boxed areas (in schematics at right) indicate the site in the LGN where the photomicrographs were taken.

of EphA-electroporated ferrets (**Figs. 4b** and **5d–f**). Indeed, the degrees of ipsilateral eye axon mistargeting and intermingling of binocular projections caused by EphA overexpression were similar in magnitude to the most extreme cases observed after complete retinal activity blockade from P1 to P10 (refs. 9,20) (**Fig. 4b–d**). Qualitatively, however, the effects of Eph-A overexpression were somewhat different than those caused by retinal activity blockade; retinal activity blockade resulted in axons from the ipsilateral eye extending much farther than normal across both the anterior-posterior (retinotopic) and outer-inner (eye-specific) axes of the LGN[9,15,20] (**Fig. 4c**). Overexpression of EphAs, on the other hand, misdirected RGC axons primarily along the outer-inner axis of the LGN, perpendicular to eye-specific layers. In activity-blocked ferrets, the degree of expansion of the ipsilateral eye territory was approximately equal along the two axes, resulting in an ipsilateral region of larger size, but with the same aspect ratio, as that of control animals (**Fig. 4e**). In contrast, EphA-transfected animals showed a large expansion along the outer-inner axis, but very little expansion along the anterior-posterior axis, resulting in a significantly lower aspect ratio (**Fig. 4e**). We also directly compared the degree of ipsilateral eye axon expansion along the anterior-posterior axis in control, EphA-electroporated and activity-blocked ferrets. In the EphA group, ipsilateral eye axons extended over slightly more of

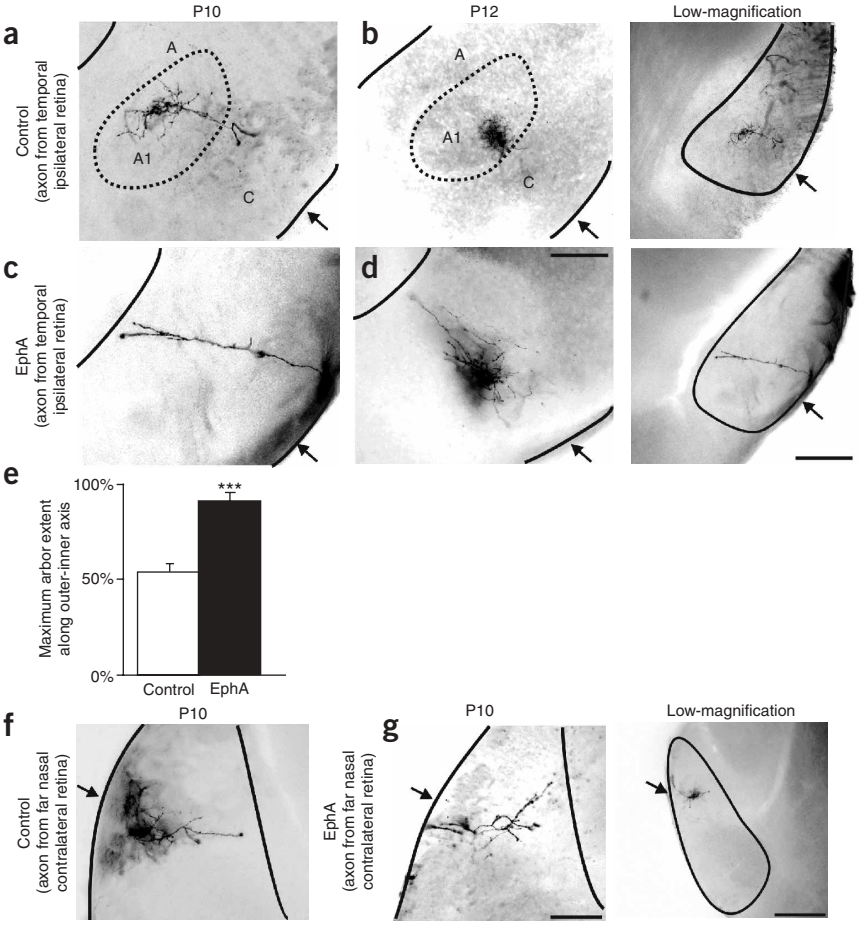

Figure 6 Effects of EphA overexpression on targeting of individual retinogeniculate axons. (**a**,**b**) RGC axons labeled from the far temporal retina of (**a**) a control P10 ferret and (**b**) a control P12 ferret, seen in the ipsilateral LGN. Low-magnification photomicrographs show the location within the LGN where axons were imaged (corresponds to same case as in **a**). Arrows indicate the optic tract. (**c**,**d**) RGC axons labeled from the far temporal retina of (**c**) a P10 EphA5-transfected (binocular electroporation) ferret and (**d**) a P12 EphA5-transfected (binocular electroporation) ferret, in the ipsilateral LGN. Low-magnification image corresponds to **c**. (**e**) Quantification of the maximum extent of the outer-inner axis in which axons from the ipsilateral retina are found. Axons from EphA animals projected significantly farther inward than did those from controls ($n = 7$ control; $n = 7$ binocular EphA5; $^{***}P < 0.005$, paired t-test). (**f**) RGC axon originating from the far-nasal retina of a control-transfected ferret, seen within the anterior portion of the contralateral LGN. (**g**) RGC axon labeled from the far nasal retina of an EphA5-electroporated ferret (binocular) seen in the anterior portion of the contralateral LGN. Low-magnification image shows nasal axon in the anterior LGN from an additional control. (**a**–**g**) Scale bar, 200 μm. In low-magnification images, scale bar = 400 μm. Horizontal plane is shown.

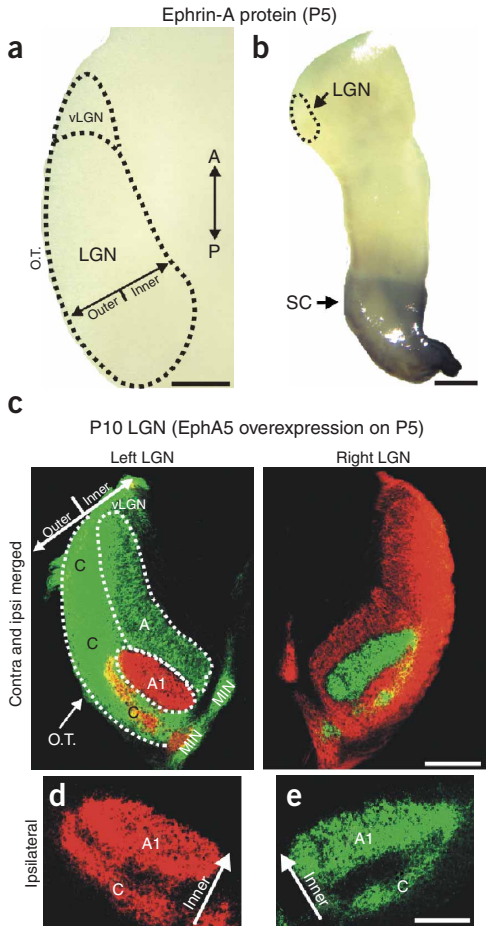

Figure 7 Ephrin-A expression in the ferret LGN is developmentally regulated. Whereas ephrin-As are robustly expressed in the P1–P3 LGN (**Fig. 1**), by P5 (**a**) they are absent. EphA3-AP was used to detect all ephrin-A ligands; the same downregulation was seen using *in situ* hybridization for ephrin-A5 mRNA (data not shown). Scale bar, 150 μm. (**b**) Low-magnification view of one side of the P5 ferret thalamus shows that, whereas ephrin-A labeling is absent from the LGN (dashed lines), ephrin-As remain high in the SC of the same tissue section. Scale bar, 250 μm. (**a**,**b**) Horizontal sections are shown. (**c**–**e**) Binocular or monocular EphA5 overexpression at ages P5 and older had no detectable effect on eye-specific retinogeniculate segregation. (Tissue from an animal subjected to binocular electroporation is shown.) Normal eye-specific layers were evident in all P5 EphA-electroporated ferrets examined ($n = 6$ ferrets; $n = 3$ EphA5; two binocular, one monocular; $n = 3$ EphA3; two binocular, one monocular). (**c**) Scale bar, 150 μm. (**d**,**e**) High-magnification views of ipsilateral eye layers in the left (**d**) and right (**e**) LGN of a P10 ferret that was electroporated with EphA5 on P5. (**d**,**e**) Scale bar, 75 μm.

the anterior-posterior axis of the LGN than in controls (control mean = 48.1 ± 1.25%; $n = 12$; EphA mean = 55.5 ± 2.4%, $n = 14$), an effect that was statistically significant ($P < 0.05$; unpaired t-test). In the activity-blocked group, ipsilateral eye axons were found over a much greater extent of the anterior-posterior axis when compared to control or EphA animals (activity block mean = 88.25 ± 1.9%, $n = 12$, $P < 0.001$ for activity blockade versus control and activity blockade versus EphA). In sum, EphA overexpression in the ferret induced drastic eye-specific pathfinding errors along the outer-inner axis of the LGN (**Fig. 6**) and significant but relatively less severe retinotopic errors along the anterior-posterior axis. Activity blockade seems to severely alter both eye-specific and retinotopic pathfinding.

EphA overexpression perturbs individual axon targeting

Whole-retina anterograde tracing of RGC axons shows the macroscopic organization of eye-specific projections to the LGN, but it cannot show whether individual ganglion cell axons make targeting errors within regions containing predominantly same-eye axons, nor can it indicate whether individual axons are displaced primarily along a single axis. Therefore, we traced individual axons arising from RGCs in defined retinotopic locations within the retina. As expected[2,38], in every control P10 ferret examined, RGC axons from the temporal portion of the retina were restricted to layer A1 within the ipsilateral LGN (**Fig. 6a**). At P12, temporal retina RGC axon arborizations formed a more restricted termination zone within A1, presaging the formation of on-off sublamination[38] (**Fig. 6b**). By contrast, in P10 and P12 ferrets that had been electroporated with EphA5 on P1, RGC axons arising from the temporal retina extended much farther along the outer-inner axis of the LGN (**Fig. 6c**,**d**). In half of the cases examined ($n = 4$), axons terminated all the way at the innermost limit of the LGN (**Fig. 6c**). In the remaining cases there was a dense terminal zone formed midway along the outer-inner axis of the LGN, but axon terminals could also be seen projecting ectopically into the inner LGN (**Fig. 6d**). Neither pattern was ever seen in control ferrets of these ages. Quantification showed that ipsilateral projecting axons in the LGN of EphA-electroporated ferrets terminated significantly further inward along the outer-inner axis of the LGN (**Fig. 6e**).

Does EphA overexpression cause targeting errors only in the binocular region of the LGN where axons from the two eyes compete? Normally, axons from the far-nasal retina project to the anterior portion of the contralateral LGN (**Fig. 6f**), which never receives axons from the ipsilateral eye[2,20]. In P10 ferrets that were electroporated with EphA5 on P1, axons from the far nasal retina were correctly targeted to the anterior contralateral LGN (**Fig. 6g**) ($n = 5$ control; $n = 7$ EphA far nasal axons). Thus, EphA overexpression seems to cause eye-specific targeting errors only in the posterior portion of the LGN where axons from the two eyes converge, consistent with a competition-based model for ephrin signaling[29,43].

Ephrin-As are developmentally regulated in the LGN

Ephrin-As were robustly expressed in the P0–P3 LGN (**Fig. 1**), but by P5 their levels were reduced conspicuously (**Fig. 7a**). This was not a false negative, because ephrin-A expression remained high in the SC and inferior colliculus of the same tissue sections where no LGN label was seen (**Fig. 7b**). Retinal EphAs, on the other hand, were stably expressed until P10 in the central > peripheral pattern described above (data not shown). To determine whether the presence of ephrin-As in the LGN is necessary for EphA overexpression to affect eye-specific pathfinding, we electroporated ferrets with EphA3/5 on P5 or P10. Despite robust overexpression of EphA3/5 in RGCs (data not shown), there was no effect on eye-specific projections to the LGN (**Fig. 7c**–**e**) ($n = 6$ ferrets). This indicates that interactions between retinal EphAs and target-derived ephrin-As are critical for eye segregation.

DISCUSSION

The results presented here are, to our knowledge, the first direct evidence for axon guidance cue–mediated targeting of eye-specific projections. Our data indicate an outer > inner gradient of ephrin-A ligand that extends along the axis of projection in the LGN. In addition, along a given line of projection, the RGCs that project to the inner LGN (layer A) express higher levels of EphAs than do the RGCs that project to the more outer LGN (layer A1). Based on the fact that

ephrin-A ligands repel RGC axons expressing relatively higher levels of EphAs[24–30,43], these ephrin-A:EphA distributions ensure that axons from the contralateral retina will project to the inner LGN and that axons from the ipsilateral retina will project to the more outer LGN. Overexpressing EphAs forced axons from the ipsilateral retina inward, into territory normally occupied only by the contralateral eye. Contralateral eye axons were mistargeted within the binocular region of the LGN as well. The targeting errors we observed following EphA overexpression were similar in magnitude to those observed following complete retinal activity blockade from P1 to P10, which is remarkable given that overexpression was induced on a background of an endogenous central > peripheral retinal EphA gradient. Our data indicate that precise levels and distributions of retinal EphAs are important for normal eye-specific pathfinding.

Developmentally regulated expression of ephrin-As

Ephrin-As are rapidly downregulated in the postnatal ferret LGN and EphA overexpression leads to disruptions in eye-specific layering only when ephrin-As are present in the LGN. Previous experiments[20,44] showed that delaying the onset of eye-specific segregation until after P10 permanently abolishes normal patterning of eye-specific inputs to the LGN, indicating that there is a critical period for development of this feature. The present data suggest that temporally restricted expression of ephrin-As within the LGN may regulate this critical period.

Because eye-specific segregation occurs gradually from P1 to P10 in the ferret[2], we were at first surprised to see downregulated ephrin-As in the LGN by P5. In mice too, however, ephrin-As are downregulated in the LGN and SC prior to the retraction of RGC axons to their retinotopically appropriate locations[28,29]. It remains unknown why ephrin-A downregulation occurs before axon targeting is complete.

Eye-specific versus retinotopic pathfinding

The ephrin-A expression patterns and the effects of EphA overexpression we describe here directly implicate these molecules in eye-specific retinogeniculate targeting. The effects of EphA overexpression on retinotopic pathfinding, however, were relatively minor in comparison. This is likely because, in ferrets, retinotopic mapping occurs prenatally, before the onset of eye-specific segregation[34–36]. Ephrin-As may well mediate retinotopic mapping in the ferret, but this is likely to occur at earlier developmental ages than we consider here. Indeed, over 40 years ago, it was proposed that, in animals with a high degree of binocular vision, a central > peripheral gradient of a mapping cue would be present in the retina to induce retinotopic mapping of nasal and temporal RGC axons to the same line of projection[45]. We thus suspect that the central > peripheral gradient of retinal EphAs we observed acts in combination with an anterior > posterior gradient of ephrin-A in the prenatal ferret LGN to accomplish this. Unfortunately, examining the pattern of ephrin-A expression in the prenatal ferret LGN has not been possible because of the extremely small size of the nucleus at the relevant ages.

In mice, retinotopy and eye-specific segregation emerge during the same developmental period and eye-specific layers do not obey the contralateral:nasal, ipsilateral:temporal distinction; RGCs from throughout the entire retina project contralaterally[32]. Thus, in mice, disrupting ephrin-As should alter both retinotopy and patterning of eye-specific layers, and indeed this is the case[28,46].

Do neural activity and ephrin-As interact?

Altering neural activity has repeatedly been shown to disrupt eye-specific patterning in the LGN[8–12]. However, there is debate regarding whether the effects observed in those experiments are caused by disruptions in Hebbian plasticity at retino-geniculate synapses or whether they are nonspecific 'permissive' effects of the activity manipulations[15]. Activity manipulation can strongly affect RGC axon outgrowth[47] and pathfinding[48], both of which could indirectly impact eye-specific segregation. In theory, activity manipulations could also act permissively by perturbing EphA expression. However, this has not been observed; normal EphA and ephrin-A mRNA expression persists in the face of chronic epibatidine application[46]—a treatment that markedly alters eye-specific retinogeniculate pathfinding in mice[11] and ferrets[9,15,20]. Its is also noteworthy that altering retinal activity causes RGC axons to extend both anteriorly and across the outer-inner axis of the LGN[9,15,20], whereas overexpression of EphAs misdirects RGC axons more along the outer-inner axis of the LGN, perpendicular to eye-specific layers (**Figs. 4–6**).

It is unlikely that the phenotype we observed following EphA overexpression reflects alterations in RGC activity levels; if overexpression of EphAs reduced or eliminated RGC activity, then in monocularly electroporated ferrets, the nontransfected eye would have expanded its projection to the LGN at the expense of the transfected eye[9,12]. This was never the case. Monocular electroporation always resulted in an expansion of axons ipsilateral to the EphA transfected eye (**Fig. 5b**). We also directly tested whether EphA overexpression affects spontaneous retinal activity by recording from RGCs using multi-site extracellular recordings in P3, P5 and P7 ferret retinal explants. Those experiments confirmed that normally patterned spontaneous retinal activity is present in EphA-electroporated retinas; at every age examined, 'waves'[9,44] of excitation periodically emerged and spread laterally across restricted domains of the retina, engaging closely spaced RGCs to fire in synchrony (**Supplementary Figs. 2–4**, **Supplementary Table 1** and **Supplementary Movies 1,2**). No significant differences were evident in the correlation strengths measured in control versus EphA-electroporated retinas at any age (**Supplementary Figs. 2–4** and **Supplementary Table 1**). The presence of normal correlated retinal activity patterns indicates that the effects of EphA overexpression on retinogeniculate pathfinding are not due to eliminating or disrupting spontaneous retinal activity. Rather, they reflect direct actions of ephrin-As and EphAs on RGC axon targeting in the LGN.

Non-ephrin-A contributions to eye-specific targeting

Our ephrin-A model does not address eye-specific segregation in the C layers because in ferrets, eye specificity within the C layers is not well established anatomically until roughly P20 (ref. 2). Mapping of RGC inputs to the C layers may rely on ephrins and/or other cues. Microarray-based genetic screens have shown the presence of molecular markers that distinguish between the C and A/A1 layers of the ferret LGN[49], but whether those molecules mediate RGC axon pathfinding remains untested. Our data do not rule out the possibility of axon guidance molecules expressed strictly in the contralateral versus ipsilateral eye layers of the LGN. Others have attempted to identify genes differentially expressed in layer A versus A1 of the ferret LGN and did not find evidence for such markers. They therefore hypothesized that the cues that mediate eye-specific targeting are expressed in gradients[49]. Our findings support this hypothesis.

Differential timing of ingrowth of RGC axons from the contralateral versus ipsilateral retina could also contribute to the invariant positioning of eye-specific layers[13]. RGC axons from the contralateral eye arrive earlier in the LGN than do axons from the ipsilateral eye[16,17]. We think it is unlikely, however, that the invariant positioning of eye-specific layers is due only to differences in timing of ingrowth because modern tracing techniques show that in the P1–P3 ferret, axons from the contralateral and ipsilateral eye project to the inner limit of the

LGN[15,20]. Timing of ingrowth may, however, impart an advantage to contralateral eye axons for securing the innermost LGN through differences in arborization maturation and synaptic efficacy.

CONCLUSION

We favor a model whereby, after axons from the two eyes map to their retinotopically appropriate locations in the LGN, axons from the contralateral retina are biased to arborize at more inner LGN locations than retinotopically matched axons from the ipsilateral eye, by virtue of the relatively greater levels of EphAs they express. Ephrin-As that are present directly on RGC axons as well as on LGN cells may be important in this process[42].

METHODS

Animals. Male and female pigmented ferrets (Marshall Farms) were maintained on a 16:8 h light:dark cycle. All procedures were in compliance with approved animal protocols from University of California, Davis and US National Institutes of Health guidelines.

Affinity probe detection of ephrin-A and EphA proteins. Procedures for AP probe detection of Ephrin-A ligands and receptors were identical to those described previously[28,29,40]. For detailed procedures, see **Supplementary Methods**.

***In situ* hybridization.** Riboprobes generated from rodent-specific templates were previously shown to work well in ferrets[41]. Riboprobe templates for mouse ephrin-A5 and EphA5 were generated from early postnatal mouse SC using primers based on verified sequences from the public database at the National Center for Biotechnology and Information (NCBI, http://www.ncbi.nlm.nih.gov/).

We cloned a ferret-specific template for EphA5 from neonatal ferret superior and inferior colliculas using PCR amplification with the same primers used to generate mouse EphA5. For detailed procedures, see **Supplementary Methods**.

EphA5:V5 expression plasmid. To examine the distribution of overexpressed EphA5 in the LGN, we fused the epitope tag V5 to the C terminus of full-length EphA5. Details of this construct are available in the **Supplementary Methods**. Expressed EphA5-V5 was detected by immunocytochemistry using a monoclonal antibody against the V5 peptide (Invitrogen) at a dilution of 1:100, and secondary detection was done with goat anti-mouse Alexa 594 (Molecular Probes).

Affinity probe densitometry analysis. We quantified sections from the dorsal, mid and ventral portions of the retina (Scion Image). The midpoint along the nasal-temporal axis was aligned, scanned and scaled for length, and densitometry values were averaged. The zero point in the plot represents the half-way point between the nasal and temporal poles. Multiple retinas were examined for each age (n = 3–4 at every postnatal day from P0–P10 and on P15). Results were compared to those achieved with SEAP.

***In vivo* ganglion cell electroporation.** Full length cDNAs encoding EphA3 or EphA5 in the mammalian expression vector pcDNA3 were used. cDNAs encoding the reporter gene enhanced green fluorescent protein (EGFP; Clontech) and/or the expression vector pcDNA3 alone were used as controls and for coelectroporation experiments. We injected 2 µl of cDNA solution (1 µg/µl) into the vitreal chamber using a 33-gauge needle inserted at the corneo-scleral junction. The eye was clasped with a paddle electrode (1 × 3 mm; BTX systems). One or two 950-ms, 10- to 12-V pulses were applied (interpulse interval = 100 ms). Although longer pulse trains (5–10 pulses) with these voltages can be used with no evidence of cell death or eye damage, we consistently achieved the highest transfection efficiency by applying only 1–2 pulses.

Quantification of RGC density. Measurements of RGC density were carried out from matched locations in the central and peripheral retina of all four quadrants of age-matched control and electroporated flat-mounted retinas. Dye labeling was used to identify RGCs. Our cell counts were comparable to those reported previously[12,20,33].

Whole-retina tracing of retinogeniculate afferents. Retinogeniculate projections were labeled using previously published protocols[20]. CTβ conjugated to Alexa dye 488 (green label) was used for the right eye, and CTβ conjugated to Alexa dye 594 (red label) was used for the left eye (Molecular Probes; CTβ has no biological activity). For detailed procedures, see **Supplementary Methods** online. Ages written in this article correspond to age at time of death. All retinas were carefully inspected for damage using previously described criteria[20]. All animals exhibiting retinal damage were excluded from the study (n = 6 ferrets).

Imaging and quantification of eye-specific retinogeniculate projections. Image acquisition and quantification of the extent of ipsilateral eye axons and overlap were identical to previous reports[12,15,20]. For details of quantification of long and short axis length, aspect ratio and extent of ipsilateral eye terminations, see **Supplementary Methods** online.

Labeling and quantification of individual retinogeniculate axons. A small (~1 mm diameter) crystal of DiI (Molecular Probes) was placed in the ventrotemporal or far nasal retina of ferrets using a 33-gauge sterile needle inserted through the sclera. The animal was perfused with 4% paraformaldyhyde 48 h later, which provided time for diffusion of the DiI while the animal was still alive. A more thorough description of the single-axon labeling procedures is available online. To quantify the extent of arborization along the outer-inner axis of the LGN, the distance between the optic tract and the perigeniculate/LGN border was measured at the location of the axon arborization of interest. The inward-most termination of each temporal axon arborization was measured along this axis and expressed as a percentage for each case (to normalize for differences in the width of the LGN). Seven cases each were examined for control and EphA transfected groups.

Retinal activity blockade. Details of the activity blockade procedure have been described previously[9,15,20]. Ferrets received binocular injections of epibatidine (1–2 µl per eye;1 mM; Sigma) every 48 h from P1 to 10.

Recording spontaneous retinal activity. Retinas were isolated and submerged in buffered and oxygenated medium (Eagle's minimum essential medium, Sigma M7278; n = 2 control; n = 2 EphA5-electroporated retinas were recorded for three ages, P3, P5 and P7, for a total of 12 retinas). Isolated retinas were placed with the RGC layer side down onto a multi-electrode array[50] (Multi-Channel Systems), held in place with a piece of dialysis membrane and superfused at 1–2 ml/min at 37 °C. Simultaneous analog data were acquired from the array of 60 electrodes, and individual spike trains were then identified using Offline Sorter (Plexon) using spike amplitude and width clustering. Because many RGCs fire together during a wave event, this standard spike identification method may result in multiple cells being assigned to one spike event because spike signals overlap. For details on the procedure used for quantifying the correlation index, see **Supplementary Methods**.

Note: Supplementary information is available on the Nature Neuroscience website.

ACKNOWLEDGMENTS

We thank P. Nguyen, R. Kumar, D. Van Der List and G. Woods for technical assistance, M. Greenberg for the gift of the EphA3 and EphA5 expression plasmids and Colin Akerman for permission to adapt his ferret visuotopic map diagram. This work was supported by the US National Eye Institute (NEI; EY11369 to B.C. and EY14689-01 to D.A.F.), the NEI Vision Science Training Fellowship (EY015387 to A.D.H.), NS39094 (E.G. Jones, University of California, Davis, provided support for K.D.M.) and NEI Core Grant (EY12576 to L.M. Chalupa).

COMPETING INTERESTS STATEMENT

The authors declare that they have no competing financial interests.

Received 29 April; accepted 23 June 2005
Published online at http://www.nature.com/natureneuroscience/

1. Rakic, P. Prenatal genesis of connections subserving ocular dominance in the rhesus monkey. *Nature* **261**, 467–471 (1976).
2. Linden, D.C., Guillery, R.W. & Cucchiaro, J. The dorsal lateral geniculate nucleus of the normal ferret and its postnatal development. *J. Comp. Neurol.* **203**, 189–211 (1981).

3. Shatz, C.J. The prenatal development of the cat's retinogeniculate pathway. *J. Neurosci.* **3**, 482–499 (1983).
4. Sengpiel, F. & Kind, P.C. The role of activity in development of the visual system. *Curr. Biol.* **12**, R818–R826 (2002).
5. Jones, E.G. *The Thalamus-Revisited* (Cambridge University Press, Cambridge, UK, 2005).
6. Thompson, I. & Holt, C. Effects of intraocular tetrodotoxin on the development of the retinocollicular pathway in the Syrian hamster. *J. Comp. Neurol.* **282**, 371–388 (1989).
7. Adams, D.L. & Horton, J.C. Capricious expression of cortical columns in the primate brain. *Nat. Neurosci.* **6**, 113–114 (2003).
8. Shatz, C.J. & Stryker, M.P. Prenatal tetrodotoxin infusion blocks segregation of retinogeniculate afferents. *Science* **242**, 87–89 (1988).
9. Penn, A.A., Riquelme, P.A., Feller, M.B. & Shatz, C.J. Competition in retinogeniculate patterning driven by spontaneous activity. *Science* **279**, 2108–2112 (1998).
10. Chapman, B. Necessity for afferent activity to maintain eye-specific segregation in ferret lateral geniculate nucleus. *Science* **287**, 2479–2482 (2000).
11. Rossi, F.M. *et al.* Requirement of the nicotinic acetylcholine receptor beta 2 subunit for the anatomical and functional development of the visual system. *Proc. Natl. Acad. Sci. USA* **98**, 6453–6458 (2001).
12. Stellwagen, D. & Shatz, C.J. An instructive role for retinal waves in the development of retinogeniculate connectivity. *Neuron* **33**, 357–367 (2002).
13. Shatz, C.J. Competitive interactions between retinal ganglion cells during prenatal development. *J. Neurobiol.* **21**, 197–211 (1990).
14. Sanes, J.R. & Yamagata, M. Formation of lamina-specific synaptic connections. *Curr. Opin. Neurobiol.* **9**, 79–87 (1999).
15. Huberman, A.D. *et al.* Eye-specific retinogeniculate segregation independent of normal neuronal activity. *Science* **300**, 994–998 (2003).
16. Guillery, R.W., Polley, E.H. & Torrealba, F. The arrangement of axons according to fiber diameter in the optic tract of the cat. *J. Neurosci.* **2**, 714–721 (1982).
17. Walsh, C. & Guillery, R.W. Age-related fiber order in the optic tract of the ferret. *J. Neurosci.* **5**, 3061–3069 (1985).
18. Crowley, J.C. & Katz, L.C. Development of ocular dominance columns in the absence of retinal input. *Nat. Neurosci.* **2**, 1125–1130 (1999).
19. Crowley, J.C. & Katz, L.C. Early development of ocular dominance columns. *Science* **290**, 1321–1324 (2000).
20. Huberman, A.D., Stellwagen, D. & Chapman, B. Decoupling eye-specific segregation from lamination in the lateral geniculate nucleus. *J. Neurosci.* **22**, 9419–9429 (2002).
21. Williams, R.W., Hogan, D. & Garraghty, P.E. Target recognition and visual maps in the thalamus of achiasmatic dogs. *Nature* **367**, 637–639 (1994).
22. Guillery, R.W. & Kaas, J.H. A study of normal and congenitally abnormal retinogeniculate projections in cats. *J. Comp. Neurol.* **143**, 73–100 (1971).
23. Guillery, R.W., Scott, G.L., Cattanach, B.M. & Deol, M.S. Genetic mechanisms determining the central visual pathways of mice. *Science* **179**, 1014–1016 (1973).
24. Cheng, H.J., Nakamoto, M., Bergemann, A.D. & Flanagan, J.G. Complementary gradients in expression and binding of ELF-1 and Mek4 in development of the topographic retinotectal projection map. *Cell* **82**, 371–381 (1995).
25. Drescher, U. *et al.* In vitro guidance of retinal ganglion cell axons by RAGS, a 25 kDa tectal protein related to ligands for Eph receptor tyrosine kinases. *Cell* **82**, 359–370 (1995).
26. Nakamoto, M. *et al.* Topographically specific effects of ELF-1 on retinal axon guidance in vitro and retinal axon mapping *in vivo*. *Cell* **86**, 755–766 (1996).
27. Frisen, J. *et al.* Ephrin-A5 (AL-1/RAGS) is essential for proper retinal axon guidance and topographic mapping in the mammalian visual system. *Neuron* **20**, 235–243 (1998).
28. Feldheim, D.A. *et al.* Topographic guidance labels in a sensory projection to the forebrain. *Neuron* **21**, 1303–1313 (1998).
29. Feldheim, D.A. *et al.* Genetic analysis of ephrin-A2 and ephrin-A5 shows their requirement in multiple aspects of retinocollicular mapping. *Neuron* **25**, 563–574 (2000).
30. Feldheim, D.A. *et al.* Loss-of-function analysis of EphA receptors in retinotectal mapping. *J. Neurosci.* **24**, 2542–2550 (2004).
31. Godement, P., Salaun, J. & Imbert, M. Prenatal and postnatal development of retinogeniculate and retinocollicular projections in the mouse. *J. Comp. Neurol.* **230**, 552–575 (1984).
32. Herrera, E. *et al.* Zic2 patterns binocular vision by specifying the uncrossed retinal projection. *Cell* **114**, 545–557 (2003).
33. Cucchiaro, J.B. Early development of the retinal line of decussation in normal and albino ferrets. *J. Comp. Neurol.* **312**, 193–206 (1991).
34. Jeffery, G. Retinotopic order appears before ocular separation in developing visual pathways. *Nature* **313**, 575–576 (1985).
35. Jeffery, G. Shifting retinal maps in the development of the lateral geniculate nucleus. *Brain Res. Dev. Brain Res.* **46**, 187–196 (1989).
36. Chalupa, L.M. & Snider, C.J. Topographic specificity in the retinocollicular projection of the developing ferret: an anterograde tracing study. *J. Comp. Neurol.* **392**, 35–47 (1998).
37. Johnson, J.K. & Casagrande, V.A. Prenatal development of axon outgrowth and connectivity in the ferret visual system. *Vis. Neurosci.* **10**, 117–130 (1993).
38. Hahm, J.O., Cramer, K.S. & Sur, M. Pattern formation by retinal afferents in the ferret lateral geniculate nucleus: developmental segregation and the role of N-methyl-D-aspartate receptors. *J. Comp. Neurol.* **411**, 327–345 (1999).
39. Sretavan, D.W. & Shatz, C.J. Prenatal development of retinal ganglion cell axons: segregation into eye-specific layers within the cat's lateral geniculate nucleus. *J. Neurosci.* **6**, 234–251 (1986).
40. Flanagan, J.G. *et al.* Alkaline phosphatase fusions of ligands or receptors as *in situ* probes for staining of cells, tissues, and embryos. *Methods Enzymol.* **327**, 19–35 (2000).
41. Hayes, S.G., Murray, K.D. & Jones, E.G. Two epochs in the development of gamma-aminobutyric acidergic neurons in the ferret thalamus. *J. Comp. Neurol.* **463**, 45–65 (2003).
42. Hornberger, M.R. *et al.* Modulation of EphA receptor function by coexpressed ephrinA ligands on retinal ganglion cell axons. *Neuron* **22**, 731–742 (1999).
43. Brown, A. *et al.* Topographic mapping from the retina to the midbrain is controlled by relative but not absolute levels of EphA receptor signaling. *Cell* **102**, 77–88 (2000).
44. Muir-Robinson, G., Hwang, B.J. & Feller, M.B. Retinogeniculate axons undergo eye-specific segregation in the absence of eye-specific layers. *J. Neurosci.* **22**, 5259–5264 (2002).
45. Sperry, R.W. Chemoaffinity in the orderly growth of nerve fibers and connections. *Proc. Natl. Acad. Sci. USA* **50**, 703–710 (1963).
46. Pfeiffenberger, C. *et al.* Ephrin-As and neural activity are required for eye-specific patterning during retinogeniculate mapping. *Nat. Neurosci.* **8**, 1020–1025 (2005).
47. Goldberg, J.L. *et al.* Retinal ganglion cells do not extend axons by default: promotion by neurotrophic signaling and electrical activity. *Neuron* **33**, 689–702 (2002).
48. Ming, G., Henley, J., Tessier-Lavigne, M., Song, H. & Poo, M. Electrical activity modulates growth cone guidance by diffusible factors. *Neuron* **29**, 441–452 (2001).
49. Kawasaki, H., Crowley, J.C., Livesey, F.J. & Katz, L.C. Molecular organization of the ferret thalamus. *J. Neurosci.* **24**, 9962–9970 (2004).
50. Meister, M., Wong, R.O., Baylor, D.A. & Shatz, C.J. Synchronous bursts of action potentials in ganglion cells of the developing mammalian retina. *Science* **252**, 939–943 (1991).